Supplemental Data:

Supplemental Table 1: Depletion constructs used in the Manuscript

Gene Target (construct type)	Targeting Sequence	Source/Reference
Scramble	non targeting pool	dharmacon SMARTpool
RB1 (si pool)	GAAUCUGCUUGUCCUCUUA	dharmacon SMARTpool
RB1 (si pool)	AAACUACGCUUUGAUAUUG	dharmacon SMARTpool
RB1 (si pool)	GAGUUGACCUAGAUGAGAU	dharmacon SMARTpool
RB1 (si pool)	CGAAAUCAGUGUCCAUAAA	dharmacon SMARTpool
RB1 #1 (si)	GGTTGTGTCGAAATTGGATCA	(Manning et al., 2010)
RB1 #23 (si)	GAACAGGAGUGCACGGAUA	dharmacon ON-TARGETplus
RB1 #24 (si)	GGUUCAACUACGCGUGUAA	dharmacon ON-TARGETplus
RB1 #25 (si)	CAUUAAUGGUUCACCUCGA	dharmacon ON-TARGETplus
RB1 #26 (si)	CAACCCAGCAGUUCGAUAU	dharmacon ON-TARGETplus
RB1 (pINDsh)	AGCAGTTCGATATCTACTGAAA	(Meerbrey et al., 2011)
RB1 (sh#1)	CCACATTATTTCTAGTCCAAA	TRCN0000040163
RB1 (sh#2)	GACTTCTACTCGAACACGAAT	TRCN0000010418
RB1 (sh#3)	CAGAGATCGTGTATTGAGATT	TRCN0000010419
Rad21 (si)	GGUGAAAAUGGCAUUACGG	(Watrin et al., 2006)
SMC3 (si)	AUCGAUAAAGAGGAAGUUU	(Watrin et al., 2006)
hCAPD3 (si)	CAUGGAUCUAUGGAGAGUA	(Hirota et al., 2004)
Wapl (si)	CGGACUACCCUUAGCACAA	(Gandhi et al., 2006)
Wapl #9 (si)	GGAGUAUAGUGCUCGGAAU	dharmacon SMARTpool
Wapl #10 (si)	GAGAGAUGUUUACGAGUUU	dharmacon SMARTpool
Wapl #11 (si)	CAAACAGUGAAUCGAGUAA	dharmacon SMARTpool
Wapl #12 (si)	CCAAAGAUACACGGGAUUA	dharmacon SMARTpool
Mad2L1 (si pool)	UUACUCGAGUGCAGAAAUA	dharmacon SMARTpool
Mad2L1 (si pool)	CUACUGAUCUUGAGCUCAU	dharmacon SMARTpool
Mad2L1 (si pool)	GGUUGUAGUUAUCUCAAAU	dharmacon SMARTpool
Mad2L1 (si pool)	GAAAUCCGUUCAGUGAUCA	dharmacon SMARTpool

Supplemental Figures

Supplemental Figure 1 (Related to Figure 1): pRB depletion promotes defects in mitotic cohesion and chromosome segregation. For each experiment, pRB depletion was obtained using at least two of the following: a set of four pooled siRNA constructs from dharmacon (siPool), five individual siRNA constructs (siRB #1, #23, #24, #25, #26), three characterized shRNA hairpins (Sh#1, Sh#2, Sh#3), and/or a previously characterized, inducible shRNA construct (pIND-shRB). Construct sequences and citations are available in Table S1. **A)** Western blot analysis demonstrating efficient knockdown with a representative siRNA and a representative shRNA. Characterization of individual si- and shRNA constructs demonstrates that pRB-depletion with each similarly **B)** compromises mitotic cohesion (increases inter-kinetochore distances) and **C)** promotes defects in mitotic chromosome segregation (also Manning et al., 2010; and data not shown). **D)** qPCR analysis of mRNA levels shows significant depletion of siRNA targets used throughout, where siRB and siWapl represent pooled siRNA constructs (siPool) targeting each respective gene. **E)** Approximately 25% of anaphase cells depleted of pRB with the siPool exhibit lagging chromosomes, compared to only 5% of control cells. Error bars represent the standard deviation between experimental replicates. **F)** Representative image of a lagging chromosome in an anaphase pRB-depleted cell (white arrow head). Kinetochores (Hec1) in green, tubulin in red, and DAPI in blue. **G)** Examples of additional anaphase defects, though less frequent (% of anaphase cells indicated for each), are apparent following pRB depletion. These defects include the presence of chromatin bridges and acentromeric DNA fragments. Staining for the DNA

damage marker gH2AX (green in this panel) reveals that pRB-deficient anaphase cells exhibit DNA damage at telomeres, near erroneously attached kinetochores (ACA: in orange), and on acentrosomal DNA fragments. Inset shows 4X enlargement of a merotelic attachment with associated DNA damage. **H)** DAPI staining reveals that prometaphase cells depleted of pRB exhibit a decrease in chromatid arm cohesion.

Supplemental Figure 2 (Related to Figure 1): pRB loss but not changes in Mad2 protein levels contribute to defects in chromatin structure A) Fluorescence in situ hybridization (FISH) with probes specific for 16p13 (green) and 16q22 (red) were used to quantify S phase cohesion (distance between replicated foci of the same color) in control, pRB, cohesin (Rad21 and SMC3) and condensin II (CAPD3) –depleted cells. Cohesin depleted cells, but not condensin depleted cells resulted in decreased S phase cohesion similar to that seen in pRB-depleted RPE cells (*: $p<0.01$). pRB depletion similarly decreased both **B)** chromatid cohesion and **C)** compaction in HCT 116 cells. **D)** qPCR was used to determine mRNA levels of pRB and Mad2L1 36 hr following pRB depletion. There is no increase in Mad2 levels following acute depletion of pRB. **E)** Western blot analysis of Mad2 and pRB levels confirm knockdown efficiency and show there is no obvious change in Mad2 protein levels. **F)** Western blot analysis showing high levels of expression can be achieved by transient transfection with an mCherry-Mad2. **G-I)** FISH analysis with probes for chromosome 16p13 and 16q22, and measures of inter-kinetochore distance in cells overexpressing mCherry-Mad2 (as described in Figure 1) reveal that acute overexpression (24h-36h) of Mad2 is not sufficient to induce changes in

S phase chromatin structure or mitotic centromeric structure. Error bars represent standard deviation between experimental replicates.

Supplemental Figure 3 (Related to Figure: 2): Cells exhibit various cohesin-linked defects following pRB loss. A) qPCR measures of mRNA levels confirm efficiency of pRB siRNA knockdown and show upregulation of p107, a characterized E2F1 target. However, no significant change is observed in various characterized regulators of cohesin function. **B) C & D)** Control and pRB-depleted S/G2 cells were fixed and stained for the DNA damage marker γH2AX (green), tubulin (red) and DAPI (blue). Cells exhibiting >5 foci were considered positive for damage. pRB depleted cells were nearly twice as likely to exhibit DNA damage than control depleted cells. **E & F)** DNA double strand breaks were induced with Hoechst/UV treatment in control and pRB-depleted cells (damaged region in upper half of each panel: γH2AX in green, DAPI in blue). Following extraction, cells were fixed and stained for chromatin associated cohesin (SMC3 in red) and the fluorescence intensity of cohesin was scored for all γH2AX positive nuclei, revealing that cohesin enrichment on chromatin following DNA damage in pRB-depleted cells was compromised. **G & H)** Following sensitization by growth in BrdU, a UV laser was used to induce localized stripes of double strand breaks. Cells were then extracted, fixed and stained for the DNA damage marker γH2AX. Recruitment of γH2AX to stripes of damage was enhanced in cells lacking pRB, consistent with published work showing cohesin limits γH2AX spreading (Caron et al., 2012). B) Measures of total γH2AX signal, normalized to the length of the stripe length (intensity/stripe) shows that both the range of γH2AX intensity as well as the average intensity is increased in pRB-depleted calls, and

these changes are comparable to that seen in Rad21 depleted cells. Bold lines indicate median intensity/length for each condition, lesser lines indicate the 1st and 3rd quartile (Ctrl vs -RB: p=0.0016; -RB vs –Rad21: p=0.9943). **I)** Chromatin immunoprecipitation (ChIP) assays using antibodies specific for H4K20 trimethylation reveal that neither condensin II (CAPD3), nor cohesin (SMC3) depletion alters the abundance of this mark at pericentromeric heterochromatin.

Supplemental Figure 4 (Related to Figure 3): Wapl depletion and nucleoside addition promote chromatin association of cohesin. A) Cells were pre-extracted, then fixed and stained for cohesin (Rad21) and kinetochores (ACA). Immuno-fluorescent analysis showed that depletion of Wapl was sufficient to promote cohesin association with mitotic chromosomes in cells depleted of pRB. **B)** Cell fractionation was performed on asynchronously dividing control (Ctrl) and pRB-depleted (siR) cells that were either co-depleted of Wapl (siW), or supplemented with nucleosides (+n). Western blot analysis showed that Wapl depletion, but not nucleoside addition was sufficient to enhance global cohesin (SMC3 and Rad21) chromatin association in both control and pRB-depleted cells. **C)** Western blot analysis of cell lysates was used to assess SMC3 acetylation in control and pRB-depleted cells following Wapl co-depletion or nucleoside addition. Both Wapl depletion and nucleoside addition restore SMC3 acetylation in pRB-depleted cells to levels comparable to that seen in either condition alone (siWapl or +nucl). **D)** qPCR analysis of mRNA levels confirmed that loss of pRB enhances expression of cell cycle genes (E2F1 and Cyclin E). Co-depletion of Wapl, or addition of nucleosides does not suppress the enhanced expression of these genes following pRB loss. **E)** qPCR analysis

confirms efficient mRNA depletion of Wapl 24 hours post-transfection with a panel of siRNA constructs targeting Wapl alone, or in combination with those targeting pRB. **F)** Analysis of anaphase cells reveals that each siWapl construct similarly suppresses lagging chromosomes that result from pRB depletion.

Supplemental Figure 5 (Related to Figure 4): Promoting cohesin stability suppresses replication defects. Cells were pulse labeled with nucleotide analogs, DNA combing assays were performed, nucleotides were detected by indirect immunofluorescence and fiber lengths were measured for pRB-depleted cells **A)** co-depleted of Wapl or **B)** treated with nucleosides. Both conditions suppressed replication defects and allowed fiber growth comparable to that seen in control cells treated with scrambled siRNA. Fibers from both siRBsiWapl cells, and those from siRB+nucleosides cells were comparable to that in control cells ($p=0.026$ and 0.079 for siRB/siWapl and siRB/+nuc respectively v Ctrl). **C & D)** DNA fiber assays performed in SAOS2 cells revealed that both Wapl depletion and nucleoside addition similarly promote replication (3.602μm and 4.507μm respectively; $p=0.0012$). **E)** pRB depletion in BJ fibroblasts **F)** leads to an increase in nucleotide pools (Ctrl vs shRB#2 or shRB #3: $p< 0.005$ for each nucleotide). This is in contrast to a proposed model that inhibition of pRB function leads to replication defects due to limiting pools of nucleotides (Bester et al., 2011).

Supplemental Figure 6 (Related to Figure 5): Neither replication defects nor corruption of Condensin II are sufficient to explain CIN in pRB-depleted cells. Induction of replication stress is insufficient to mimic defects seen in pRB-depleted cells.

A) To determine the impact of replication stress on chromosome segregation, RPE cells were treated with varying concentrations of HU and allowed to proliferate in the presence of drug overnight. Cells were than fixed, stained, and scored for the presence of anaphase defects including lagging chromosomes and anaphase bridges. Cells treated with 0.1mM HU displayed anaphase defects comparable to that seen in pRB depleted cells. However, these same concentrations of HU are insufficient to **B)** alter cohesin acetylation (WB analysis) or **C)** chromatid cohesion (FISH assay). Nucleosides feed into many different metabolic pathways and the nucleoside supplements likely impact many nuclear events. As such, it remains possible that nucleoside rescue works in pRB-deficient cells because it improves rates of replication in other manners, independent of effects on nucleotide pools, such as via effects on cohesin levels/stability. **D & E)** To comparatively assess the amount of replicative stress required to induce anaphase defects presented in panel A, Cells where treated with scrambled or pRB-specific siRNA, or with varying concentrations of HU for 24 hours, then treated or not with 5mM Caffeine to compromise the G2/M checkpoint. In the absence of Caffeine, the intact checkpoint enabled all conditions to correct any replicative stress prior to mitotic entry, allowing for normal metaphase chromatin structure and alignment on the spindle. **E)** In the presence of Caffeine, the majority of control cells (siScr), which experience little replicative stress, enter mitosis normally. ~80% of cells depleted of pRB (siRB) similarly experience little replicative stress and enter mitosis normally. In the presence of Caffeine, cells experiencing increased replicative stress (increasing concentrations of HU) enter mitosis with massive cumulative stress, leading to shattered chromosomes that no longer associate with kinetochore structures and can not align along the metaphase plate

(representative image in D). Concentrations of HU that produce a comparable level of cumulative replication stress (0.05mM HU) are insufficient to induce anaphase defects at rates seen in pRB-depleted cells. Together this suggests that the cohesion changes in in pRB-depleted cells reflect a specific property of pRB inactivation, rather than a general consequence of replication stress. **F & G)** While loss of the condensin II complex via depletion of CAPD3 is sufficient to both promote anaphase lagging chromosomes and increase DNA damage on it's own, the severity of these defects following short term CAPD3 depletion precludes analysis of a potential additive relationship between pRB and CAPD3 co-depletion. However, in contrast to that demonstrated in pRB-depleted cells, Wapl co-depletion from siCAPD3-treated cells is insufficient to suppress defects in mitotic fidelity or DNA damage. This suggests that suppression of mitotic defects in pRB-depleted cells by Wapl co-depletion is independent of any role Condensin II may play in these processes.

Figure S1:

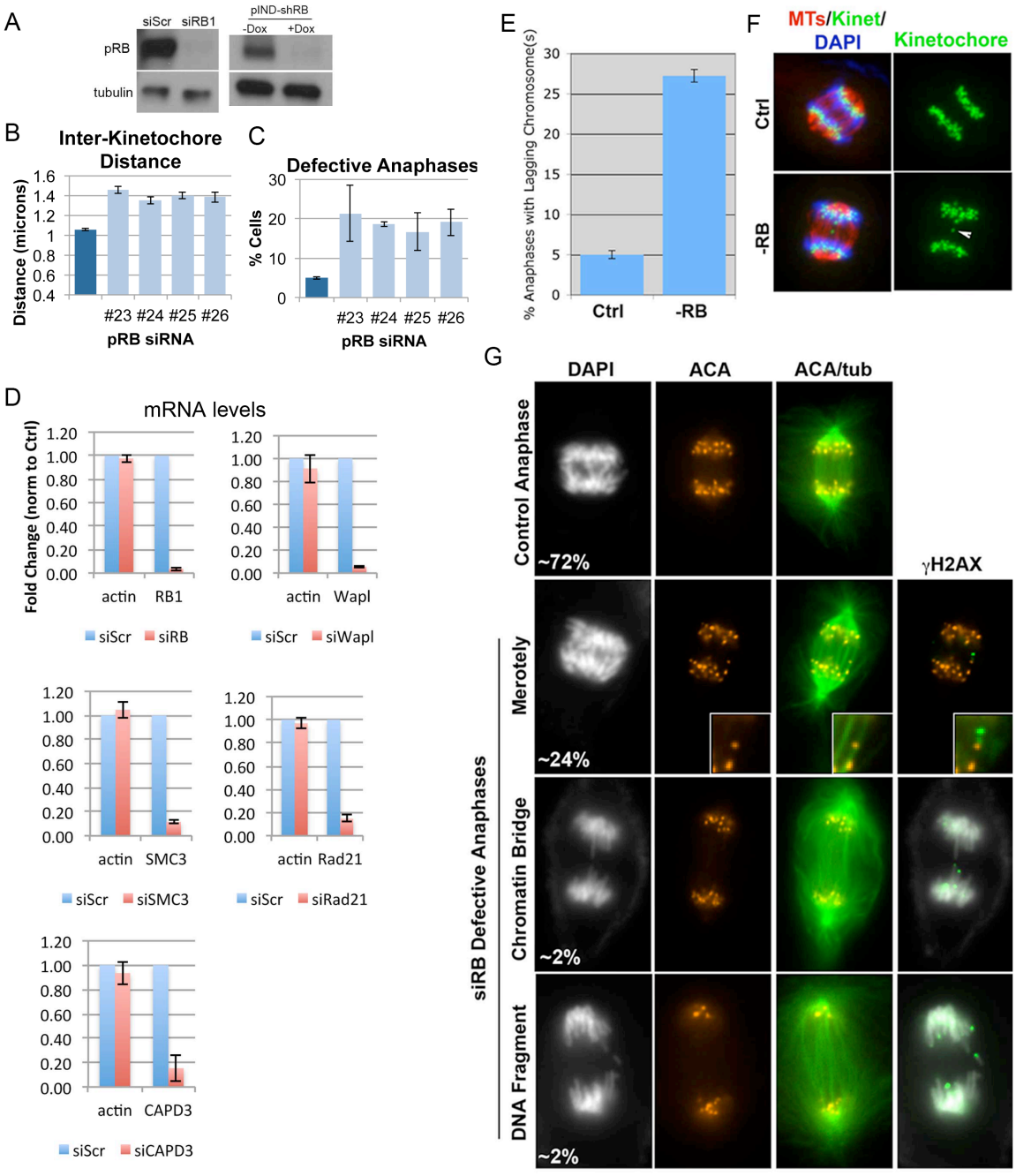

H

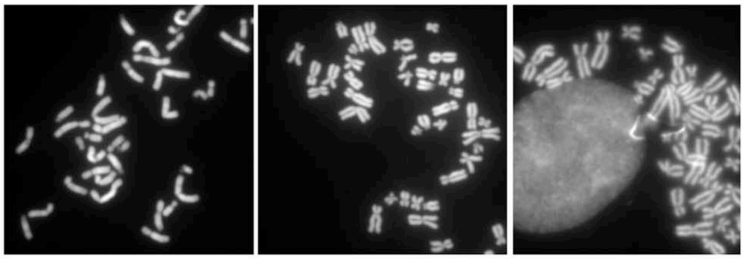

	% Cells	
	Tight	Loose
siScr	96	4
siRB	56	44

Figure S2:

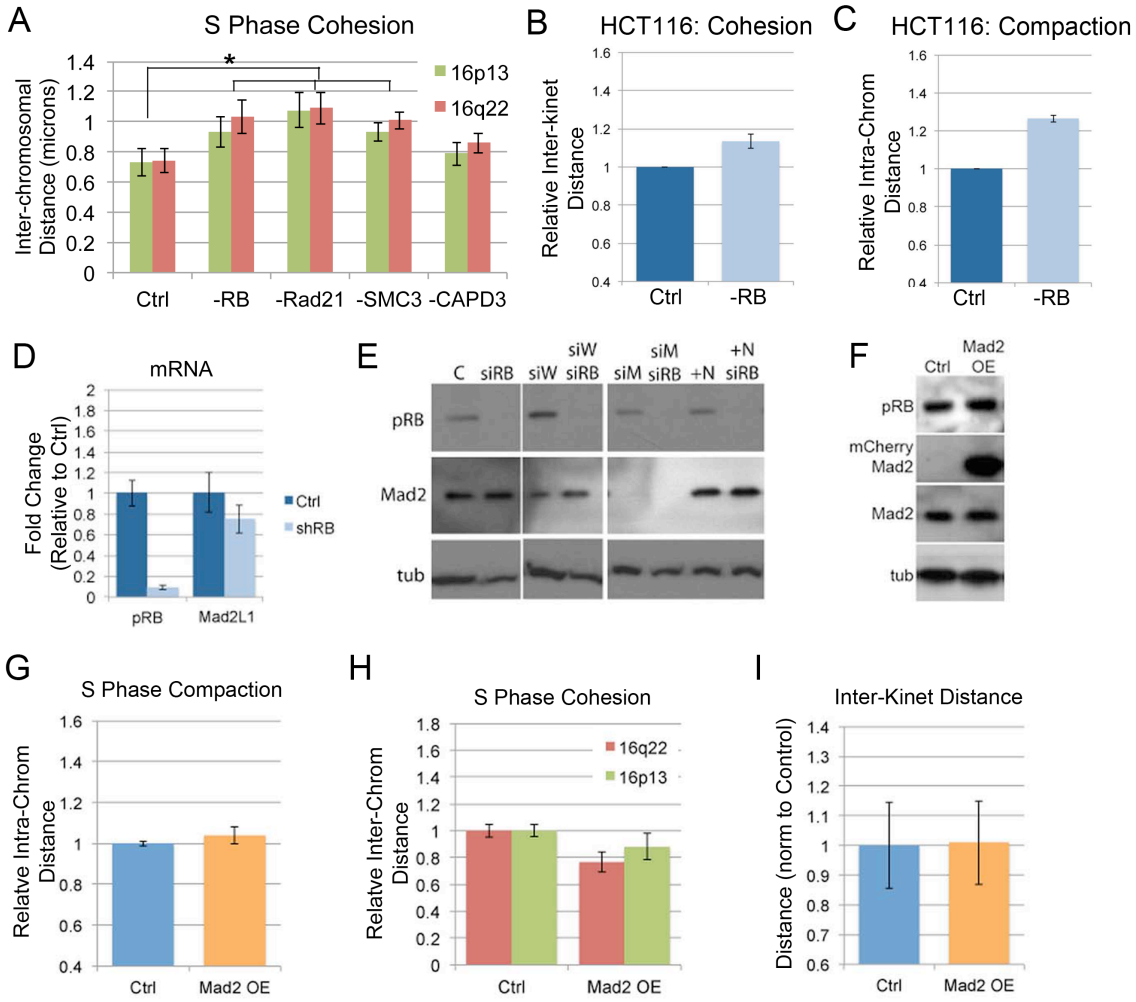
A
S Phase Cohesion
Inter-chromosomal Distance (microns)
16p13
16q22
Ctrl
-RB
-Rad21
-SMC3
-CAPD3
B
HCT116: Cohesion
Relative Inter-kinet Distance
Ctrl
-RB
C
HCT116: Compaction
Relative Intra-Chrom Distance
Ctrl
-RB
D
mRNA
Fold Change (Relative to Ctrl)
Ctrl
shRB
pRB
Mad2L1
E
C
siRB
siW
siW siRB
siM
siM siRB
+N
+N siRB
pRB
Mad2
tub
F
Ctrl
Mad2 OE
pRB
mCherry Mad2
Mad2
tub
G
S Phase Compaction
Relative Intra-Chrom Distance
Ctrl
Mad2 OE
H
S Phase Cohesion
Relative Inter-Chrom Distance
16q22
16p13
Ctrl
Mad2 OE
I
Inter-Kinet Distance
Distance (norm to Control)
Ctrl
Mad2 OE

Figure S3:

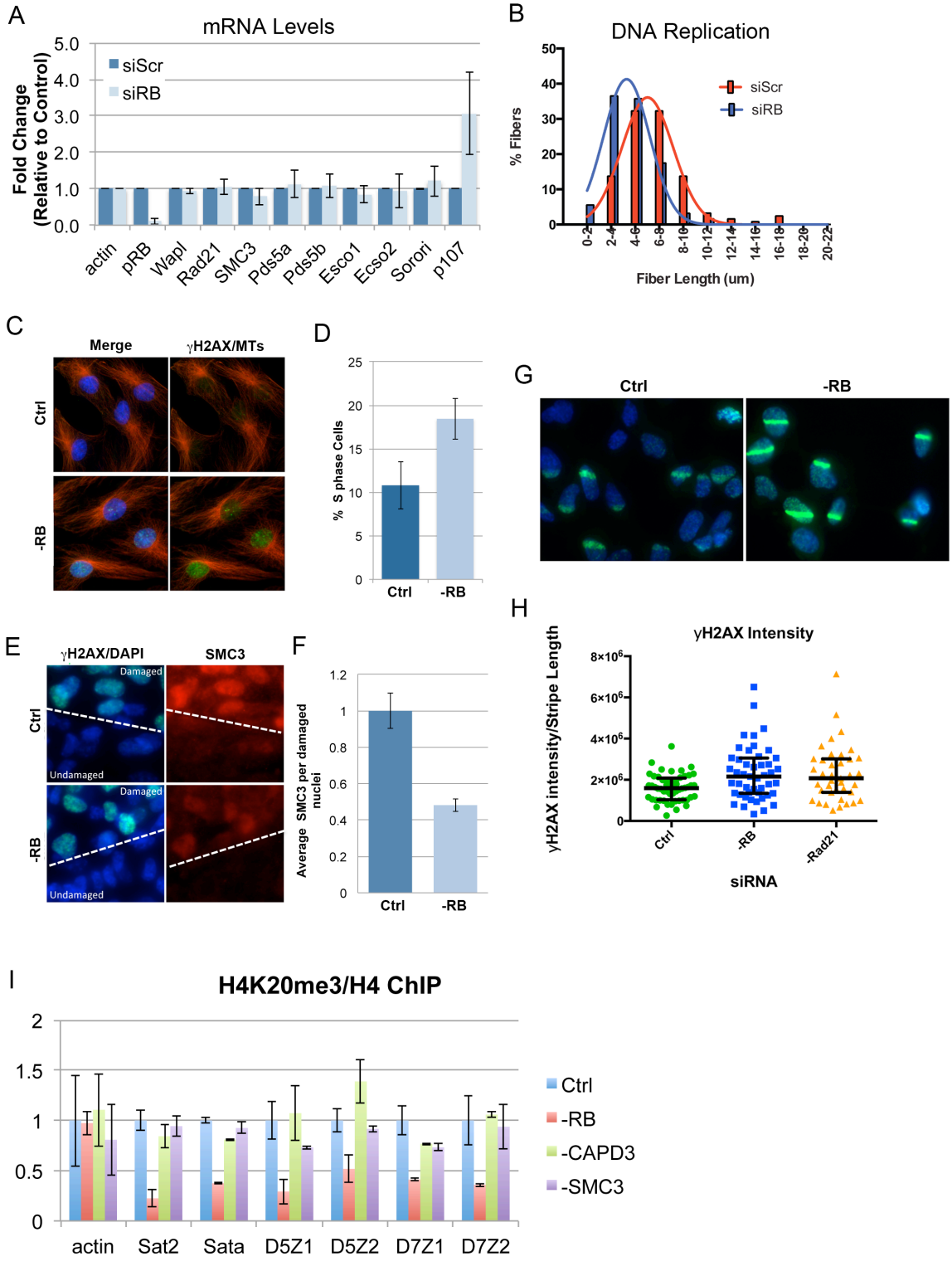
A
mRNA Levels
Fold Change (Relative to Control)
siScr
siRB
actin
pRB
Wapl
Rad21
SMC3
Pds5a
Pds5b
Esco1
Esco2
Sorori
p107
B
DNA Replication
% Fibers
siScr
siRB
Fiber Length (um)
C
Merge
γH2AX/MTs
Ctrl
-RB
D
% S phase Cells
Ctrl
-RB
G
Ctrl
-RB
E
γH2AX/DAPI
SMC3
Damaged
Undamaged
F
Average SMC3 per damaged nuclei
H
γH2AX Intensity
γH2AX intensity/Stripe Length
siRNA
-Rad21
I
H4K20me3/H4 ChIP
-CAPD3
-SMC3
Sat2
Sata
D5Z1
D5Z2
D7Z1
D7Z2

Figure S4

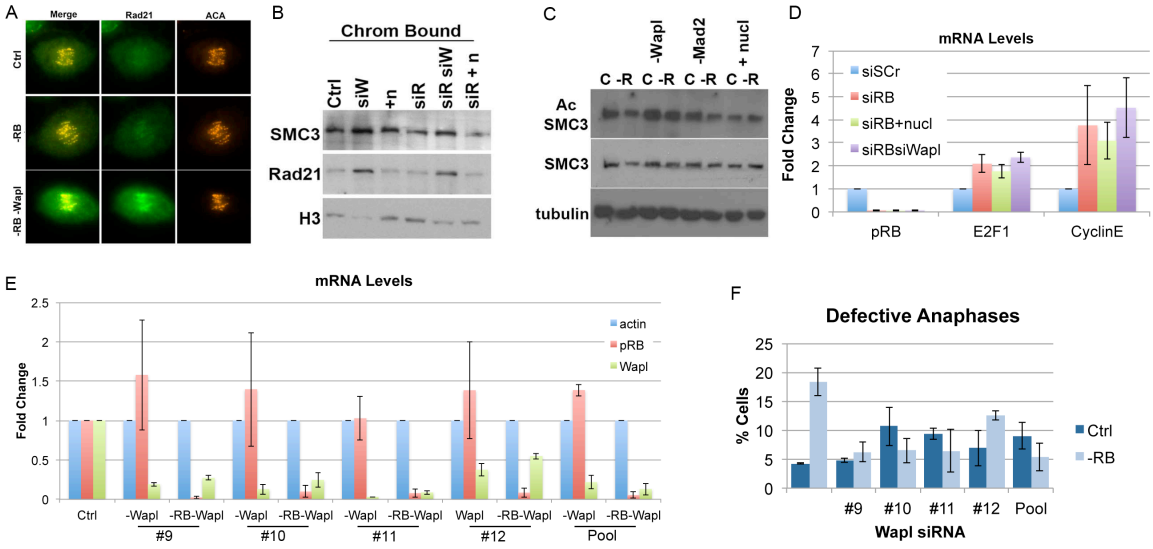
A
Merge
Rad21
ACA
Ctrl
-Rb
-Rb -Wapl
B
Chrom Bound
Ctrl
siW
+n
siR
siR siW
siR + n
SMC3
Rad21
H3
C
-Wapl
-Mad2
+ nucl
C -R C -R C -R C -R
Ac SMC3
SMC3
tubulin
D
mRNA Levels
siSCr
siRB
siRB+nucl
siRBsiWapl
Fold Change
pRB
E2F1
CyclinE
E
mRNA Levels
actin
pRB
Wapl
Fold Change
Ctrl
-Wapl
-RB-Wapl
#9
#10
#11
#12
Pool
F
Defective Anaphases
% Cells
Ctrl
-RB
#9
#10
#11
#12
Pool
Wapl siRNA

Figure S5:

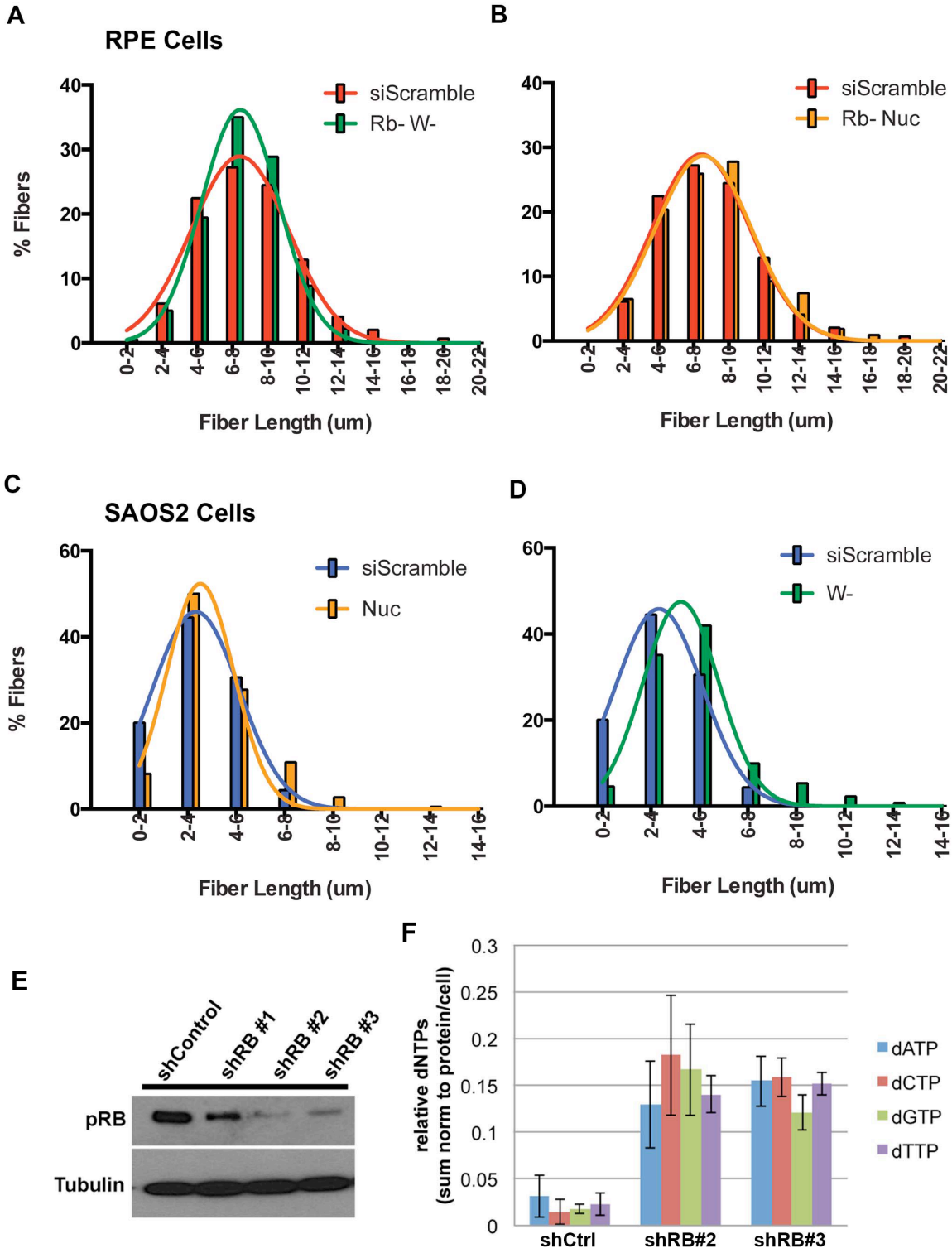
A
RPE Cells
siScramble
Rb- W-
% Fibers
Fiber Length (um)
B
siScramble
Rb- Nuc
Fiber Length (um)
C
SAOS2 Cells
siScramble
Nuc
% Fibers
Fiber Length (um)
D
siScramble
W-
Fiber Length (um)
E
shControl
shRB #1
shRB #2
shRB #3
pRB
Tubulin
F
relative dNTPs (sum norm to protein/cell)
dATP
dCTP
dGTP
dTTP
shCtrl
shRB#2
shRB#3

Figure S6:

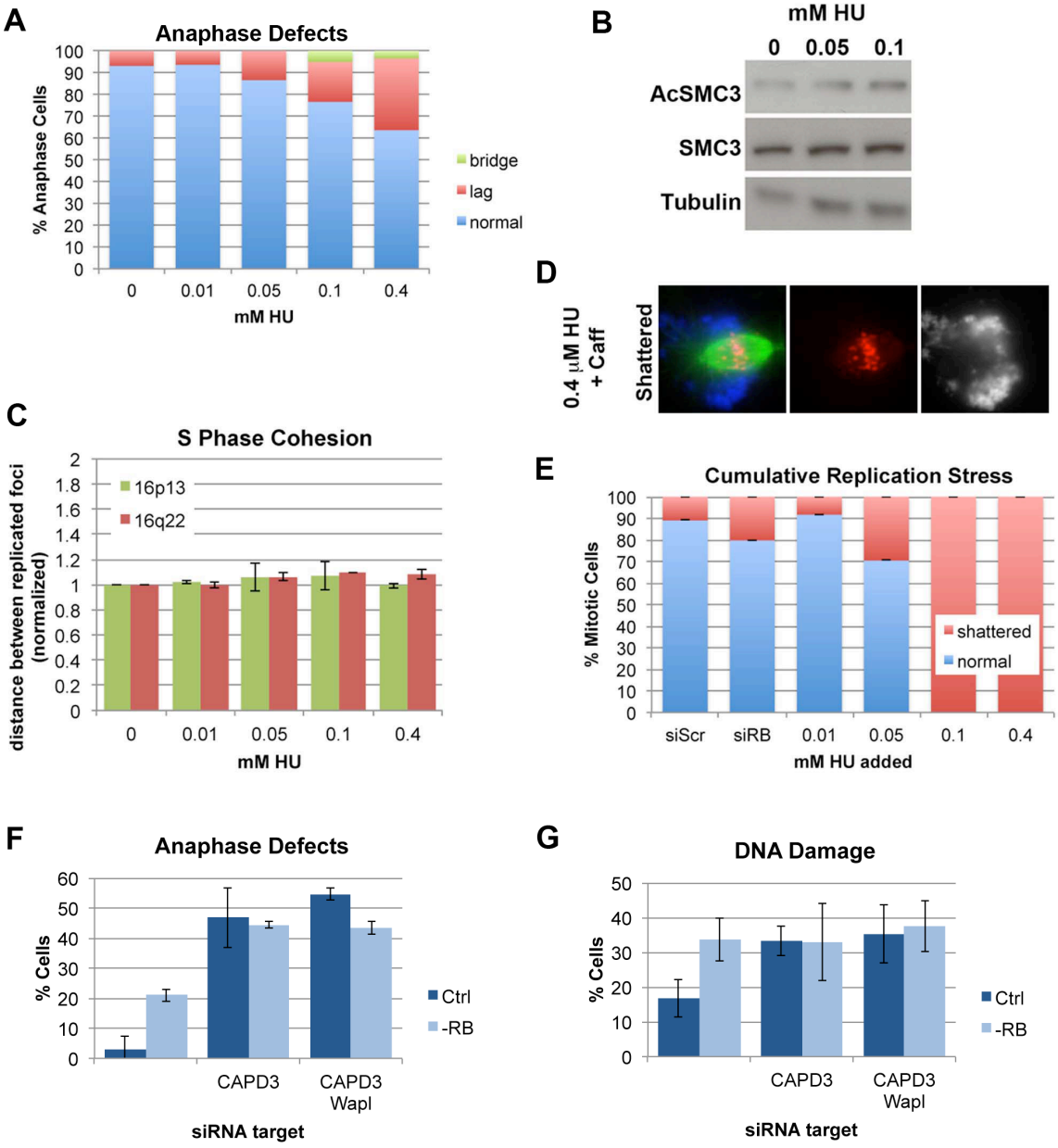
A
Anaphase Defects
% Anaphase Cells
mM HU
bridge
lag
normal
B
mM HU
0 0.05 0.1
AcSMC3
SMC3
Tubulin
C
S Phase Cohesion
distance between replicated foci (normalized)
16p13
16q22
mM HU
D
0.4 μM HU + Caff
Shattered
E
Cumulative Replication Stress
% Mitotic Cells
shattered
normal
siScr
siRB
mM HU added
F
Anaphase Defects
% Cells
Ctrl
-RB
CAPD3
CAPD3 Wapl
siRNA target
G
DNA Damage
% Cells
Ctrl
-RB
CAPD3
CAPD3 Wapl
siRNA target

Supplemental Materials and Methods:

Cell culture

hTERT-RPE-1 (RPE) cells, hTERT-BJ cells (BJ) and SAOS-2 cells were grown in Dulbecco's Modified Essential Medium (DMEM) supplemented with 10% fetal bovine serum and 1% penicillin/streptomycin. HCT116 cells were grown in McCoy's medium supplemented with 10% fetal bovine serum and 1% penicillin/streptomycin. All cells were cultured at 37C and 5% CO2.

Immunofluorescence microscopy and Antibodies

Cells were fixed for 10 min in ice cold methanol (ACA [Antibodies Inc], Ndc80/Hec1[Novus Biologicals], α-tubulin [Sigma]) or alternatively pre-extracted in microtubule stabilizing buffer (4 M glycerol, 100mM PIPES pH 6.9, 1mM EGTA, 5mM MgCl2, 0.5% Triton X-100) followed by fixation in 4% Paraformaldehyde for 20 min (SMC3 [Bethyl Labs]). When imaging of γH2AX (Cell Signaling, Millipore) foci was performed, cells were additionally post-extracted in PBS + 0.5% Triton X-100 for 10 min. Blocking, antibody incubations and subsequent washes were performed in TBS-BSA (10mM Tris pH 7.5, 150 mM NaCl, 1% bovine serum albumin). DNA was detected with 0.2 μg/mL DAPI. Coverslips were mounted with ProLong Antifade mounting medium (Molecular Probes) and fluorescent images were captured with a Hamamatsu EM CCD camera mounted on an Olympus IX81 microscope with either a 40x or 100x, 1.4NA objective. A series of 0.5 or 0.25-μM optical sections were captured in the Z-axis with each objective, respectively. Selected planes for the Z-series were then overlaid to generate the final image. For identification of Anaphase defects, DAPI, tubulin, and

kinetochore staining was analyzed. Measurements of inter-kinetochore distance were made with Slidebook analysis software. For each assay, measurements were performed of > 50 cells per condition for each of three independent experiments. Error bars represent standard deviation between replicates. The Student's two-tailed t-test was used to calculate the significance between samples. Additional antibodies used for western blot analysis include: Acetylated SMC3 (A generous gift from Katsuhiko Shirahige), Histone 3 (abcam), Mad2 (Covance), RB1 (4H1: Cell Signaling), Rad21 (Upstate), SMC3 (Bethyl), and SMC1 (Bethyl).

Fluorecence *in situ* hybridization (FISH)

Cells were prepared, fixed and hybridized with probes as previously described (Manning et al., 2010). FISH probes were purchased from Cytocell and were designed to be specific for the α-satellite regions of chromosomes 2, 6, 8, or Chr16p13 and Chr16q22 as indicated. Measures of both inter-chromosomal distances (arm cohesion) and intra-chromosomal distances (compaction) were performed with Slidebook analysis software. Cell cycle stage for cohesion and compaction measurements were based on the presence of absence of replicated FISH foci, together with DAPI staining: nuclei with single foci indicated G1, intact nuclei with replicated foci indicated S/G2. Cells were treated with 100ng/mL colcemid for 4 hours to induce mitotic arrest and enable mitotic measures of chromosome arm compaction, unless indicated otherwise. Cells were treated with 1μM hydroxyurea, or 2 mM Thymidine for 20 hours to inhibit replication and induce S phase arrest. Three independent replicates, with at least 50 measurements per condition, were performed for compaction and cohesion assays. For measures of chromosome copy

number, at least 100 cells were scored for each of 3 replicates, per condition. To determine the rate of segregation errors in SAOS cells, control, Wapl-depleted or nucleoside-treated cells were plated sparsely on glass coverslips and allowed to compete <1 cell cycle prior to fixation and preparation for FISH analysis of chromosome copy number. For each condition, >300 individual segregation events were scored. Only divisions in which all copies of the analyzed chromosome could be accounted for were scored.

Induction of DNA damage

To induce DNA damage, cells were pre-sensitized with Hoescht for 30 min or labeled with BrdU overnight, a region of the coverslip was then exposed to UV light. Measurements of chromatin-bound cohesin by immunofluorescence were performed with Slidebook software by selecting nuclei based on γH2AX staining and/or DAPI, and measuring total pixel intensity of cohesin staining within the selected regions. An Arcturus Veritas Laser Capture Microsdisection System was used with a UV laser setting of 0.25 UV to induce stripes of DNA damage in Hoescht-treated cells. Laser striping experiments were performed on cells grown in glass chamber slides (Fisher Scientific), with experimental conditions plated adjacent to one another to ensure timing following damage was consistent between samples. Laser striping was performed sequentially, with < 2min between samples, samples were fixed 1 hour following damage induction. Approximately 50 cells were analyzed per condition for each of four independent replicates.

ChIP assay

Chromatin immunoprecipitations were performed on RPE cells stably expressing a doxycycline-inducible shRB construct. 10 cm plates of dishes were induced with 2 μg/mL doxycycline or not for 48h to express shRB and additionally transfected with control scrambled siRNA, Wapl siRNA, Halo-Suv4-20 (Black et al., 2013) or treated with 50 nM nucleosides as described above. At 36 hours post-transfection and induction, cells were crosslinked with 1% formaldehyde for 15 min, followed by addition of 0.125 M Glycine for 5 min. Cells were collected, washed in cold PBS and re-suspended in Cellular Lysis Buffer (5 mM PIPES, 85mM KCl, 0.5% NP40) for 5 min on ice. Cells were collected, re-suspended in Nuclear Lysis Buffer (50 mM Trisp pH8, 10mM EDTA pH8, 0.2% SDS) and sonicated for 1 h 15 min at 60% power for 40/20 sec on/off intervals in a Qsonica water bath sonicator to generate chromatin fragments ~500bp. Sonicated chromatin extract was diluted 10-fold in IP buffer (16.7 M Tris pH8, 1.2 M EDTA, 167 mM NaCl, 0.01% SDS, 1.1% Triton X100), incubated overnight with 2 μg Rad21 (abcam), H4K20me1 (abcam), H4K20me3 (abcam) antibody or control IgG, then immunoprecipitated with protein A or protein G coated magnetic beads (Invitrogen). Beads were subsequently washed 2X in IP buffer, and 1X each in TSE (20 mM Tris pH8, 2 mM EDTA pH8, 500 mM NaCl, 1% Triton X100, 0.1% SDS), LiCl (100 mM Tris pH8, 500 mM LiCl, 1% deoxycholic acid, 1% NP40) and TE (10 mM Tris pH8, 1 mM EDTA pH8) buffers. Samples were eluted and crosslinks reversed by incubation in Elution Buffer (50 mM NaHCO3, 140 mM NaCl, 1% SDS) and 10 μg Proteinase K for 1 h at 55C, followed by 4 hours at 65C, then addition of 200 μg RNaseA and incubation at 37C for 1 h. DNA was purified with Qiagen's PCR cleanup columns.

Immunoprecipitated material was quantitated by qPCR using a Roche LC480 and FastStart Universal SYBR Green Master mix (Roche).

DNA Fiber Assays

Cells were labeled with CldU (100 uM) for 30min, washed, and labeled with IdU (250 uM) for 30min. DNA fibers were spread as described (Jackson and Pombo, 1998). Briefly, 2.5ul of the cells suspended in PBS (~10^6cell/ml) was spotted on to a glass slide and allowed to dry. 7.5ul of spreading buffer (0.5% SDS, 200mM Tris-HCl pH7.4, 50mM EDTA) was dropped on the dried cells and incubated for 10min. Slides were tilted (~15°) to allow lysed cell mixture to slowly run down the slide. Slides were air dried, fixed in methanol:acetic acid (3:1) for 3min, and stored at 4°C overnight before staining. Fibers were denatured in 2.5M HCl for 30min and blocked in 2% BSA/ 0.05% Tween for 1hr at 37°C. Detection of CldU and IdU tracts was carried out using Rat-anti-BrdU (OBT0030, AbDSerotec) (1:100) and Mouse anti-BrdU (BD Biosciences) (1:50) 1hr at 37°C, followed by Alexa-488 anti-mouse (1:100) and Cy3-Anti Rat (Jackson ImmunoResearch) (1:100) 30min 37°C. Slides were washed in PBS and mounted using VectaShield (Vector labs). Fibers were imaged at 40X with a Zeiss Axio Observer inverted microscope and Metamorph software for acquisition. Statistics were performed using a two-tailed Mann-Whitney test with Prism 6 (GraphPad) software.

dNTP quantification

dNTP levels were measured as previously described (Nicolay et al., 2013). Briefly, hTERT expressing human foreskin fibroblasts (BJ-5ta) were grown in DMEM media

(25mM Glucose, 2mM Glutamine, 50 units/mL Penicillin, 50 ug/mL Streptomycin, 10% FBS). 200,000 cells carrying the specified stably integrated shRNAs were seeded in 10cm^2 plates in biological quadruplicates (three sample replicates + one parallel plate for cell counts/protein quantification). Cells were allowed to proliferate until ~80% confluency was reached. dNTPs were extracted and identified by LCMS/MS as described previously (Nicolay et al G and D 2013). dNTPs were quantified by internally normalizing raw peak area values from each biological replicate to the sum of all metabolites measured (A total of 258 were measured). Following normalization to the sum, values were then normalized by the total protein/cell/plate. Values shown reflect the arbitrary units derived from normalization. Error bars represent the 95% confidence interval of the samples.

Supplemental References:

Bester, A.C., Roniger, M., Oren, Y.S., Im, M.M., Sarni, D., Chaoat, M., Bensimon, A., Zamir, G., Shewach, D.S., and Kerem, B. (2011). Nucleotide deficiency promotes genomic instability in early stages of cancer development. Cell *145*, 435-446.

Black, J.C., Manning, A.L., Van Rechem, C., Kim, J., Ladd, B., Cho, J., Pineda, C.M., Murphy, N., Daniels, D.L., Montagna, C.*, et al.* (2013). KDM4A Lysine Demethylase Induces Site-Specific Copy Gain and Rereplication of Regions Amplified in Tumors. Cell *154*, 541-555.

Caron, P., Aymard, F., Iacovoni, J.S., Briois, S., Canitrot, Y., Bugler, B., Massip, L., Losada, A., and Legube, G. (2012). Cohesin protects genes against gammaH2AX Induced by DNA double-strand breaks. PLoS genetics *8*, e1002460.

Gandhi, R., Gillespie, P.J., and Hirano, T. (2006). Human Wapl is a cohesin-binding protein that promotes sister-chromatid resolution in mitotic prophase. Current biology : CB *16*, 2406-2417.

Hirota, T., Gerlich, D., Koch, B., Ellenberg, J., and Peters, J.M. (2004). Distinct functions of condensin I and II in mitotic chromosome assembly. Journal of cell science *117*, 6435-6445.

Manning, A.L., Longworth, M.S., and Dyson, N.J. (2010). Loss of pRB causes centromere dysfunction and chromosomal instability. Genes & development *24*, 1364-1376.

Meerbrey, K.L., Hu, G., Kessler, J.D., Roarty, K., Li, M.Z., Fang, J.E., Herschkowitz, J.I., Burrows, A.E., Ciccia, A., Sun, T.*, et al.* (2011). The pINDUCER lentiviral toolkit for

inducible RNA interference in vitro and in vivo. Proceedings of the National Academy of Sciences of the United States of America *108*, 3665-3670.
Nicolay, B.N., Gameiro, P.A., Tschop, K., Korenjak, M., Heilmann, A.M., Asara, J.M., Stephanopoulos, G., Iliopoulos, O., and Dyson, N.J. (2013). Loss of RBF1 changes glutamine catabolism. Genes & development *27*, 182-196.
Watrin, E., Schleiffer, A., Tanaka, K., Eisenhaber, F., Nasmyth, K., and Peters, J.M. (2006). Human Scc4 is required for cohesin binding to chromatin, sister-chromatid cohesion, and mitotic progression. Current biology : CB *16*, 863-874.